Microstructural Influences Caused by Different Aging Strategies on the Strain-Dependent Damping of the High-Strength Aluminum Alloy AA7075

Steffen Lotz [1,2,*], **Jiali Zhang** [3], **Emad Scharifi** [1], **Roland Morak** [4], **Ursula Weidig** [1], **Jürgen Göken** [5], **Christoph Broeckmann** [3] and **Kurt Steinhoff** [1]

1   Metal Forming Technology, University of Kassel, Kurt-Wolters-Straße 3, 34125 Kassel, Germany
2   METAKUS Automotive GmbH, Fehrenberger Straße 1a, 34225 Baunatal, Germany
3   Institute for Materials Applications in Mechanical Engineering, RWTH Aachen, Augustinerbach 4, 52062 Aachen, Germany
4   Research and Development, AMAG Rolling GmbH, Postfach 32, 5282 Ranshofen, Austria
5   Faculty of Maritime Sciences, University of Applied Sciences Emden/Leer, Bergmannstraße 36, 26789 Leer, Germany
*   Correspondence: steffen.lotz@uni-kassel.de; Tel.: +49-(0)561-804-1944

Abstract: The present study focused on the influence of different aging conditions on the strain-dependent damping of the high-strength aluminum alloy AA7075. For this purpose, different artificial aging strategies were carried out after solution heat treatment with subsequent water quenching to identify correlations between microstructural evolution, hardness development, and individual material damping. The resulting material damping was measured using an experimental setup based on the principle of electromagnetic feedback. Scanning transmission electron microscopy (STEM) investigations were carried out using a scanning electron microscope (SEM) to characterize the material's microstructure. Depending on the aging conditions, the damping investigations revealed specific characteristic behaviors in the strain-dependent range from 1×10^{-7} to 0.002. Peak aging conditions showed lower damping than the overaged conditions but resulted in the highest hardness. The hardness decreased with increasing aging time or temperature.

Keywords: high strength aluminum alloys; strain-dependent damping; precipitation hardening

1. Introduction

High-strength aluminum alloy AA7075 is widely used in the aerospace industry due to its excellent strength-to-weight ratio combined with its resistance to stress corrosion cracking and intercrystalline corrosion [1,2]. In addition to strength, weight, and corrosion resistance, another key aspect for its application is material damping. This mechanical property contributes to the absorption of undesirable mechanical vibrations, which constitute an issue for fatigue or noise control [3,4]. Therefore, considerable research has focused on improving the damping behavior of high-strength aluminum alloys [3–5].

Damping in metals is based on internal friction and constitutes a material property associated with the ability to dissipate mechanical vibrations into thermal energy [6]. This capacity is the result of several mechanisms, the most important of which are thermoelastic damping and microstructural effects. The influence of the microstructure is mainly based on interactions of crystallographic defects [5]. Among these mechanisms, dislocation damping is the most important in aluminum [4]. The hysteretic interaction between dislocation loops, precipitates, and solute atoms influences the energy conversion. Depending on the mobility of dislocations, the damping capacity may increase or decrease. Just as dislocations affect damping, dislocations and their interaction with other microstructural defects influence material hardness.

In the work by Updike et al. [3], the influence of reinforcements on material damping was investigated. They found that graphite continuous-fiber reinforcements contributed to an increase in the damping of the high-strength alloy AA6061. Lavernia et al. [5] showed that discontinuously-reinforced aluminum alloy metal-matrix composites revealed improved damping compared to the unreinforced condition. Xie et al. [4] focused on commercial aluminum alloys, such as AA7022 and AA6082, and investigated the influence of the precipitation condition after aging on the damping capacity. For the alloy AA6082, they found increased damping after aging, which further increased after overaging. They attributed this rise in damping by aging to a higher mobility of dislocations, which depended on the remaining solute atoms and the amount and condition of the precipitates.

Several measures exist to determine damping behavior. Lavernia et al. [5], for example, used a dynamic mechanical thermal analyzer (DMTA) to measure the damping capacity of composites by calculating the tangent of the loss angle ϕ between the material's strain response and an exciting sinusoidal stress. Xie et al. [4] determined the inverse quality factor Q^{-1} as a function of temperature from the decay of free oscillation of a torsion pendulum to characterize the damping of commercial aluminum alloys. Our investigations of the influence of different aging conditions on the damping of magnesium alloys used an experimental setup based on the principle of electro-magnetic feedback and determined damping in terms of the logarithmic decrement δ, derived from the amplitude decay of a free vibration of a one-side fixed bending beam [7,8].

Little information is found in literature about a correlation between hardness properties, microstructure evolution by aging, and damping. Considering the interest in high-strength, precipitation-hardened aluminum alloys, as well as results reporting increased damping after aging and the influence of microstructural conditions on hardness and damping, the present study investigated the influence of different aging conditions on the damping behavior and hardness evolution of the high-strength aluminum AA7075. Using the method described in ref. [7] for damping measurements the aim of the study was to elaborate the dependence between the logarithmic decrement δ, aging condition, and hardness.

2. Materials and Methods

2.1. Materials

The experimental investigations in this work were carried out on the heat-treatable, high-strength aluminum alloy AA7075 (Al-Zn-Mg-Cu), which is commonly used in the aerospace industry. The alloy was delivered by Austrian Metal AG and the experiments were conducted using the as received T6 condition as plates with a thickness of 10 mm. The chemical composition of AA7075 was characterized by optical emission spectroscopy and is listed in Table 1.

Table 1. Chemical composition of AA7075.

Chemical Elements (wt.%)	Si	Fe	Cu	Mn	Mg	Cr	Zn	Ti	Others
AA7075—as received (AR)	0.08	0.12	1.6	0.04	2.7	0.19	5.9	0.05	Balance

2.2. Experimental Setup and Program

The damping measurements were performed on an experimental setup based on the principle of electromagnetic feedback, as shown in Figure 1 [7]. The samples were cut by electrical discharge machining and manufactured as bending beams fixed at the thicker end, as shown in Figure 1c. A neodymium permanent magnet was attached to the free end to establish electromagnetic coupling with a coil system, which caused a resonance vibration of the bending beam. The determined resonance frequency of the samples was approximately 58 Hz. When the excitation was stopped, the material damping was measured in terms of the logarithmic decrement (δ), calculated from the decaying bending vibration amplitudes represented by the decaying induction voltage and measured by a

digital voltmeter. The measured voltage amplitude was converted to mechanical vibration amplitudes using a correlation function. The logarithmic decrement was obtained by

$$\delta = \frac{1}{n}\ln\left(\frac{A_n}{A_{n+1}}\right) \tag{1}$$

where n = 1,2,3, . . . and A_n is the nth amplitude of the mechanical vibration. The vibration amplitude resulted in a strain amplitude that became maximum near the specimen's location of restraint. The maximum strain amplitude (ε_{max}) near the clamped end of the sample was defined as

$$\varepsilon_{max} = \frac{3a}{2 * l^2}z' \tag{2}$$

where z' is the deflection of the bending beam out of its zero position, a is the thickness, and l the length of the bending beam. Further information about the electromagnetic coupling and determination of the correlation function can be obtained in the study by Göken and Riehemann [7].
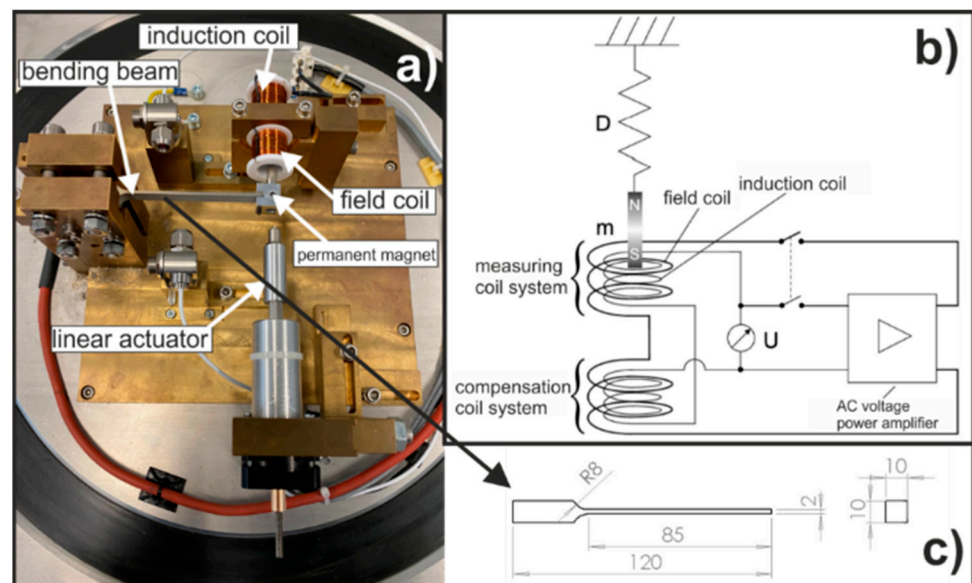
Figure 1. (**a**) Experimental setup of damping measurements; (**b**) schematic representation; (**c**) technical drawing of the sample geometry.

The material samples were first solution heat treated in a roller hearth furnace (Baettenhausen Rollmod) at 480 °C for 20 min, and then cooled in a water-dilutable polymer quenchant to achieve a high cooling rate with low thermal distortion. T4 samples were naturally aged for 80 days, while all other aging conditions were carried out using a chamber furnace (KM 70/13, Thermconcept, Bremen, Germany). The conditions and corresponding heat treatment parameters are presented in Table 2. Each heat treatment produced three samples. Three damping and five hardness measurements (Vikers) were performed on each sample. The hardness values represent the arithmetic mean of five values, while the damping values represent the arithmetic mean of three measurements.

Table 2. Heat treatment parameters for different conditions of AA7075.

Condition	T4	T6	T7-1	T7-2
Solution Heat Treatment [°C]	480	480	480	480
Aging Temperature [°C]	24	120	220	120
Aging Time	80 d	20 h	3 h	330 h

2.3. Microstructural Characterization

Microstructural analysis of the heat-treated samples were conducted using a FEI Helios Nanolab G3 CX DualBeam focused ion beam (FIB)/scanning electron microscope (SEM) (Thermo Fisher Scientific, Waltham, MA, USA). Transmission electron microscopy (TEM) lamellae were prepared following a site-specific method using FIB. Thereafter, the lamellae were imaged at an accelerating voltage of 30 kV using a scanning transmission electron microscopy (STEM) detector that was directly mounted in the DualBeam FIB/SEM.

3. Results

3.1. Damping and Hardness

Figure 2 shows the logarithmic decrement (δ) as a function of the maximum strain amplitude (ε_{max}) for all investigated conditions. With increasing strain amplitude, all samples revealed increased damping. However, there was a range of strain values in which the strain seemed to have no influence on the damping. Therefore, the curve could be divided into strain-dependent (δ_h, with "h" representing hysteretic damping) and strain-independent (δ_0) areas. The sample at the naturally aged T4 condition revealed the lowest damping, which increased continuously from the sample at the peak-aged T6 condition to that at the overaged T7-2 condition, and reached the peak value with the sample at the overaged T7-1 condition. The two overaged conditions differed in aging temperature and duration. Whilst the T7-2 condition was obtained with the same 120 °C aging temperature as the T6 condition but a 17-times longer aging duration, the T7-1 condition was obtained with a high aging temperature of 220 °C.
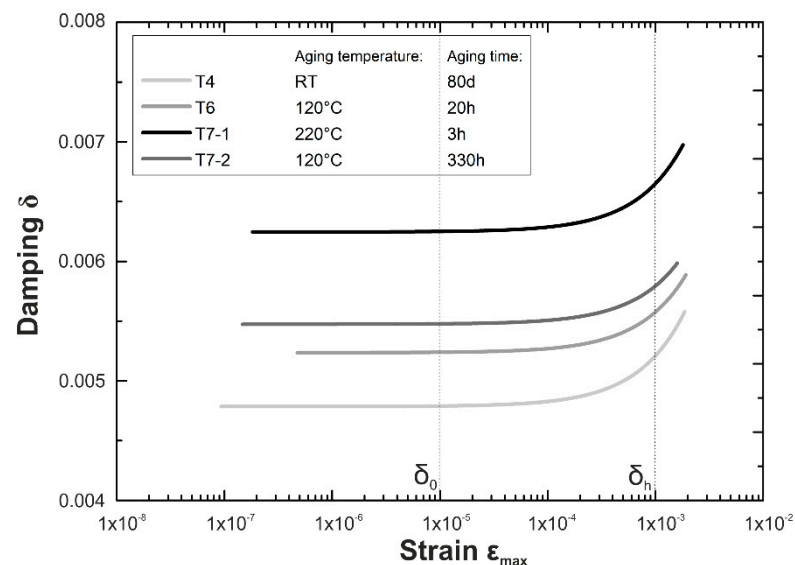
Figure 2. Strain-dependent damping measurements of the aluminum alloy AA7075.

The measured hardness of all heat treated samples is depicted in Figure 3 in comparison with the corresponding strain-dependent and strain-independent damping δ_0 and δ_h, respectively. The highest hardness level was obtained for the sample at the T6 condition (183 HV), which was artificially aged at 120 °C for 20 h. For the two overaged conditions, due to the formation of coarse precipitates, the sample at the T7-1 condition that was aged at a higher temperature of 220 °C showed a lower material hardness (93 HV) than the sample at the T7-2 condition (159 HV) that was aged at 120 °C. After natural aging for 80 days, a hardness level of 158 HV was developed that was close to the hardness of the sample at the T7-2 condition.
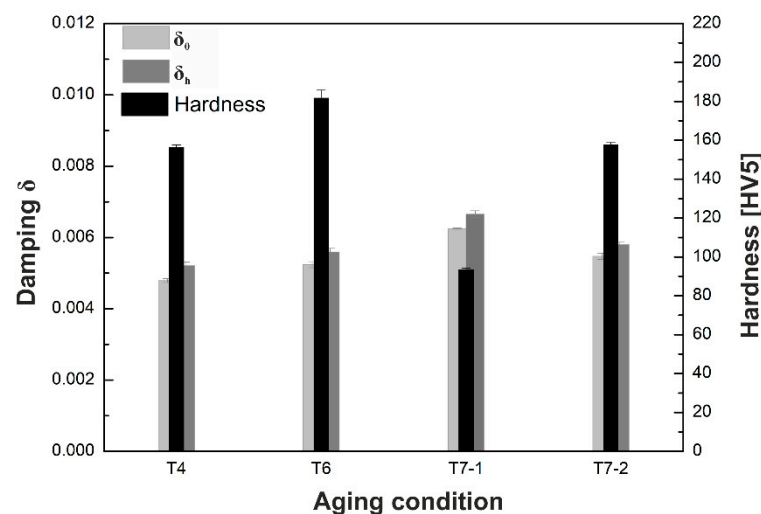
Figure 3. Damping and hardness in dependence of heat treatment condition.

3.2. Microstructural Investigation

Figure 4a,b shows the STEM images of samples at the T6 and T7-1 conditions. As expected from the adjusted heat treatment process for the T6 condition, only a few irregularly distributed and very coarse particles were observed within the grain structure (Figure 4a). The fraction of these phases was very small due to the low artificial aging temperature of 120 °C, since extensive nucleation and growth were expected at higher artificial aging temperatures. In addition, the spacing between these coarse precipitates was also very large. However, the measured high hardness level gave rise to the consideration that very fine precipitates of only a few atomic layers might exist in these zones, since they have been reported in the literature for the same material and heat treatment condition [9]. In addition to the particles in the grain interior, a few very coarse grain boundary precipitates (GB-P) were found at the grain boundary intersections (Figure 4a). On the other hand, due to the higher artificial aging temperature, a higher number of coarse precipitates, which were also larger than those of the sample at the T6 condition, were observed within the grain interior of the sample at the T7-1 condition (Figure 4b).
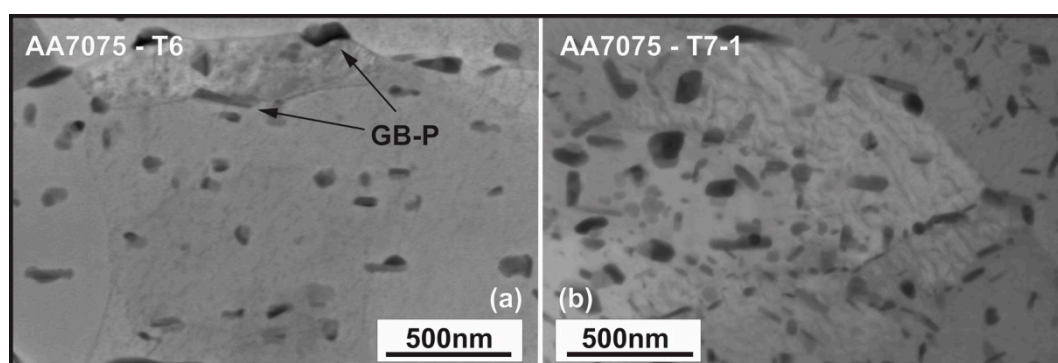
Figure 4. STEM investigation of (**a**) T6 (120 °C for 20 h) and (**b**) T7-1 (220 °C for 3 h).

4. Discussion

The effect of different aging strategies and the resulting precipitation conditions on the damping of high-strength aluminum alloy AA7075 was investigated in the present study by determining the logarithmic decrement (δ) derived from the amplitude decay of a free vibration of a one-side fixed bending beam. The damping measurements revealed a tendential increase in δ_0 and δ_h with increasing aging temperature and time. As explained in ref. [4], this behavior is mainly based on the interaction of dislocations and different

crystallographic defects in commercial aluminum alloys, such as second phases, grain boundaries, interphases, and foreign atoms. In the case of AA7075, the formation and growth of different types of clusters, e.g., Zn-rich, Mg-rich, or Cu-rich clusters, and precipitates acted as strong or weak pinning points for dislocations, depending on their size and geometry. According to the model of Granato and Lücke [10], mobile dislocations that are mainly pinned by weak pinning points generate low internal friction, whereas higher internal friction is achieved at strong pinning points. Solute atoms are considered to be weak pinning points. If the matrix is depleted of solute atoms (in the matrix or on the dislocations) due to precipitation formation, a dislocation line may bow out, resulting in increased damping [11]. Therefore, aging with increased temperature and time seems to increase material damping due to the growth of semi-coherent phases and coarse precipitates, as well as corresponding reductions in solute atoms and small particles. This investigation is valid for the peak and overaged T6 and T7-1 conditions in comparison to the T4 condition. The naturally aged T4 condition is probably the state with a high number of solute atoms and very small clusters, leading to a decrease of the dislocation loop length as well as the dislocation mobility. In contrast, the overaged T7-2 condition had a lower damping than the T7-1 condition. This may be due to a possible increase in grain size or differences in the amount and type of precipitates resulting from the differing aging temperatures and times [12–14].

The selected aging treatments also affected the hardness evolution by the same microstructural defects, which influenced the damping. The very effective precipitation hardening mechanism is responsible for the highest hardness of the sample at the T6 condition. It had the optimum amount and size of fine semi-coherent precipitates to constrain the dislocation motion. The damping was also increased; however, compared to the overaged T7-1 state, this increase was not as pronounced due to reduced dislocation mobility. Further aging led to the growth of precipitates but also to a reduction of their amount, which resulted in the observed decrease in hardness of the two overaged T7 conditions. This effect was enhanced by increased aging temperatures, which accelerated the diffusion processes. In addition, the higher temperature may have led to the formation of further precipitation phases, which may explain the lowest hardness of the sample at the T7-1 condition with the highest values of δ_0 and δ_h. The natural aging of the T4 condition produced a microstructural condition of precipitates and remaining solute atoms that resulted in a hardness close to the overaged T7-2 condition.

5. Conclusions

From the obtained results and STEM observations it can be concluded that precipitate conditions and sizes created by different aging strategies influence not only the hardness but also the internal friction, which can be revealed by damping measurements. However, no clear correlation was found between hardness and damping in the course of these investigations. Whilst the aging condition with the lowest hardness (T7-1) showed the highest damping, the condition with the highest hardness (T6) was not correlated to the lowest damping. This led to the conclusion that differences in the microstructural influence on hardness and damping are due to differences in the amount and nature of precipitates or a special precipitation formation. In addition, grain size evolution during aging may also affect damping, but this hypothesis must be investigated in further detail.

Author Contributions: Conceptualization, S.L. and U.W.; methodology, S.L., J.Z. and E.S.; investigation, S.L., J.Z. and E.S.; resources, R.M.; writing—original draft preparation, S.L. and E.S.; writing—review and editing, S.L., U.W., J.G. and K.S.; visualization, S.L. and E.S.; supervision, J.G., C.B. and K.S. All authors have read and agreed to the published version of the manuscript.

Funding: The authors would like to thank the Hessen State Ministry for Higher Education, Research and the Arts—Initiative for the Development of Scientific and Economic Excellence (LOEWE) for financial support from the project ALLEGRO (Subprojects A2 and B1).

Institutional Review Board Statement: Not applicable.

Informed Consent Statement: Not applicable.

Data Availability Statement: Not applicable.

Conflicts of Interest: The authors declare no conflict of interest.

References

1. Hornbogen, E.; Starke, E.A. Overview no. 102 Theory assisted design of high strength low alloy aluminum. *Acta Metall. Mater.* **1993**, *41*, 1–16. [CrossRef]
2. Starke, E.A.; Staley, J.T. Application of modern aluminum alloys to aircraft. *Prog. Aerosp. Sci.* **1996**, *32*, 131–172. [CrossRef]
3. Updike, C.A.; Bhagat, R.B.; Pechersky, M.J.; Amateau, M.F. The damping performance of aluminum-based composites. *JOM* **1990**, *42*, 42–46. [CrossRef]
4. Xie, C.Y.; Schaller, R.; Jaquerod, C. High damping capacity after precipitation in some commercial aluminum alloys. *Mater. Sci. Eng. A* **1998**, *252*, 78–84. [CrossRef]
5. Lavernia, E.J.; Perez, R.J.; Zhang, J. Damping behavior of discontinuously reinforced ai alloy metal-matrix composites. *Metall. Mater. Trans. A* **1995**, *26*, 2803–2818. [CrossRef]
6. Göken, J. Dämpfungspotential der Magnesiumlegierung AZ91 bei Raumtemperatur. Ph.D. Thesis, GKSS-Forschungszentrum, Geesthacht, Germany, 2003.
7. Göken, J.; Riehemann, W. Dehnungsabhängige Dämpfungsmessungen an abklingenden Biegeschwingungen von Werkstoffen. *Technol. Mess.* **2001**, *68*, 535–543. [CrossRef]
8. González-Martínez, R.; Göken, J.; Letzig, D.; Steinhoff, K.; Kainer, K.U. Influence of aging on damping of the magnesium-aluminium-zinc series. *J. Alloys Compd.* **2007**, *437*, 127–132. [CrossRef]
9. Scharifi, E.; Savaci, U.; Kavaklioglu, Z.B.; Weidig, U.; Turan, S.; Steinhoff, K. Effect of thermo-mechanical processing on quench-induced precipitates morphology and mechanical properties in high strength AA7075 aluminum alloy. *Mater. Charact.* **2021**, *174*, 111026. [CrossRef]
10. Granato, A.; Lücke, K. Theory of Mechanical Damping Due to Dislocations. *J. Appl. Phys.* **1956**, *27*, 583–593. [CrossRef]
11. Göken, J.; Riehemann, W. Dependence of internal friction of fibre-reinforced and unreinforced AZ91 on heat treatment. *Mater. Sci. Eng. A* **2002**, *324*, 127–133. [CrossRef]
12. Sajadifar, S.V.; Scharifi, E.; Weidig, U.; Steinhoff, K.; Niendorf, T. Performance of thermo-mechanically processed AA7075 alloy at elevated temperatures—From microstructure to mechanical properties. *Metals* **2020**, *10*, 884. [CrossRef]
13. Sajadifar, S.V.; Scharifi, E.; Weidig, U.; Steinhoff, K.; Niendorf, T. Effect of tool temperature on mechanical properties and microstructure of thermo-mechanically processed AA6082 and AA7075 aluminum alloys. *HTM J. Heat Treat. Mater.* **2020**, *75*, 177–191. [CrossRef]
14. Scharifi, E.; Roscher, M.; Lotz, S.; Weidig, U.; Steinhoff, K. Functional Gradation in Precipitation Hardenable AA7075 alloy by Differential Cooling Strategies. In *Key Engineering Materials*; Trans Tech Publications Ltd.: Zürich, Switzerland, 2021.